DOI:
10.1039/c4dt02965h

Document Version
Early version, also known as pre-print

Technetium-99m and rhenium-188 complexes with one and two pendant bisphosphonate groups for imaging arterial calcification

Jayanta Kumar Bordoloi [a, b], David Berry [a], Irfan Ullah Khan[a,c], Kavitha Sunassee[a], Rafael T.M. de Rosales [a], Catherine Shanahan[b], Philip J. Blower [a].

Abstract: The first ^{99m}Tc and ^{188}Re complexes containing two pendant bisphosphonate groups have been synthesised, based on the mononuclear M(V) nitride core with two dithiocarbamate ligands each with a pendant bisphosphonate. The structural identity of the ^{99}Tc and stable rhenium analogues as uncharged, mononuclear nitridobis(dithiocarbamate) complexes was determined by electrospray mass spectrometry. The ^{99m}Tc complex showed greater affinity for synthetic and biological hydroxyapatite, and greater stability in biological media, than the well-known but poorly-characterised and inhomogeneous bone imaging agent ^{99m}Tc-MDP. It gave excellent SPECT images of both bone calcification (mice and rats) and vascular calcification (rat model), but the improved stability and the availability of two pendant bisphosphonate groups conferred no dramatic advantage in imaging over the conventional ^{99m}Tc-MDP agent in which the bisphosphonate group is bound directly to Tc. The ^{188}Re complex also showed preferential uptake in bone. These tracers and the biological model of vascular calcification offer the opportunity to study the biological interpretation and clinical potential of radionuclide imaging of vascular calcification and to deliver radionuclide therapy to bone metastases.

[a] King's College London, Division of Imaging Sciences and Biomedical Engineering, St Thomas' Hospital, London SE1 7EH

[b] King's College London, Cardiovascular Division, James Black Centre, London SE5 9NU.

[c] Institute of Nuclear Medicine and Oncology (INMOL), New Campus Road, Lahore-54600, Pakistan

Dalton Discussions

PREPRINT

Introduction

Techetium-99m (^{99m}Tc) complexes of MDP (methylene diphosphonate, **1,** figure 1) and related 1,1-bisphosphonates such as HDP (hydroxymethylene diphosphonate) have been used successfully for decades in the clinic for acquiring planar and SPECT images of osteoblastic processes associated with bone tumours and metastases.[1-3] Another 1,1-bisphosphonate analogue, HEDP (**2**) has found use in palliative treatment of bone metastases with the beta-emitting rhenium isotopes rhenium-186 (^{186}Re) and rhenium-188 (^{188}Re).[4-7] Despite the proven value of these complexes in imaging and therapy, both the technetium and rhenium complexes have limitations. The structures of the active metal complexes are unknown, and certainly not homogenous.[8] Despite their periodic relationship, the technetium and rhenium complexes are not chemically analogous (for example, the technetium complexes are biologically effective at no-carrier-added concentrations whereas the rhenium complexes are ineffective without carrier non-radioactive rhenium,[9] suggesting that they are polymeric). The complexes show poor *in vivo* stability; while this is not a major problem over the short time scales of imaging with ^{99m}Tc (typically 3 h) it is detrimental to therapeutic use of $^{186/188}$Re, as a high proportion of the rhenium is rapidly converted to perrhenate[10], which does not bind to bone and is taken up in thyroid or excreted renally. The instability arises because the bisphosphonate groups in these ligands serve the dual purpose of binding the metal ion (for which they are not well-suited) and for bone targeting (in which their affinity may be compromised by the bound radiometal).

In addition to the need for improved *in vivo* stability and therapeutic efficacy of bone-targeting rhenium complexes, new applications are emerging for imaging calcification (or decalcification) processes that place more stringent demands on imaging agents than conventional imaging of osteoblastic bone metastases. For example, imaging osteolytic lesions characteristic of multiple myeloma has very poor sensitivity with conventional ^{99m}Tc-bisphosphonate complexes,[11] and imaging soft tissue calcification associated with cardiovascular diseases such as atherosclerosis and arterial calcification may require complexes with improved imaging characteristics because the lesions are small and mineral content and mineralisation/demineralisation rates may be low.

Figure 1: Bone targeting bisphosphonate derivatives for use with ^{99m}Tc and ^{188}Re.

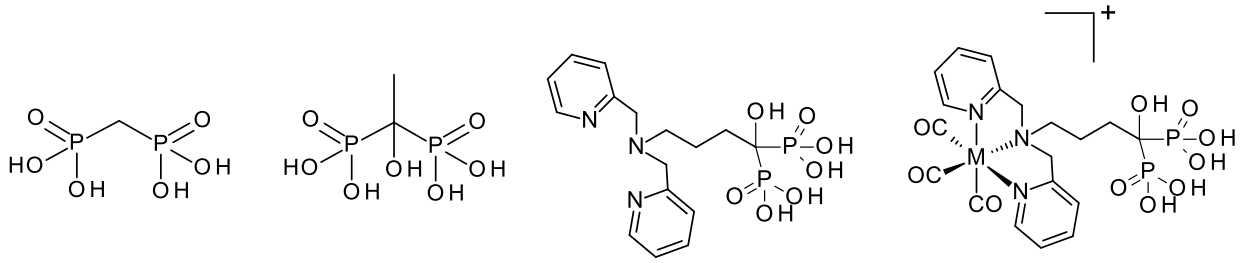

1 MDP **2** HEDP **3** DPA-Alendronate **4** $[Tc(CO)_3(DPA\text{-}Ale)]^+$ **5** $[Re(CO)_3(DPA\text{-}Ale)]^+$

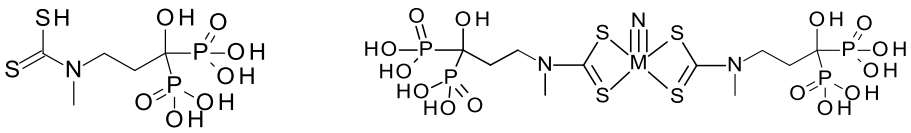

6 HDTC-BP **7** $[TcN(DTC\text{-}BP)_2]$ **8** $[ReN(DTC\text{-}BP)_2]$

To achieve the required improvements in *in vivo* stability and affinity for mineral deposits, we adopted the strategy of separating the metal chelating site from the bisphosphonate (bone targeting) site in a bifunctional molecule. This allows separate control/optimisation of metal chelation and bone targeting, exemplified by the ligand DPA-Alendronate (**3**) and its ^{99m}Tc[12] and ^{188}Re[13] complexes (**4**) using the readily-synthesised tricarbonyl $[M(CO)_3]^+$ cores. [^{188}Re]-**5** showed higher bone uptake and more prolonged bone retention of ^{188}Re *in vivo* and higher biological stability compared with ^{188}Re-HEDP (^{188}Re-**2**) over a 24 hour period.[13] The results indicate that [^{188}Re]-**5** has potential as an improved palliative agent for bone metastases, but remains non-ideal due to modest uptake in non-target organs such as the liver, attributed to the increased lipophilicity of the complex.

In this paper we extend the concept of bifunctional ligands for bone targeting, by synthesising complexes with increased mineral affinity by the inclusion of two pendant bisphosphonate groups in the molecule, and evaluating them in the challenging setting of an animal model of arterial calcification. The pentavalent technetium/rhenium nitrido bis(dithiocarbamate) core was identified as potentially meeting the requirements of retaining a structurally discrete, well-characterised and stable Tc/Re core with the expectation that the Tc and Re complexes will share similar biological behaviour. Precursors containing the $[M{\equiv}N]^{2+}$ core (M = ^{99m}Tc or ^{188}Re) are readily synthesised[14] and react with dithiocarbamates to give symmetrical $MN(DTC)_2$ complexes.[15-17] Despite the simplicity of the structures and syntheses, $MN(DTC)_2$ complexes have found only limited use in radiopharmaceuticals, amongst which ^{99m}Tc-NOET for myocardial perfusion imaging has been most prominent.[17, 18] Here we have used the ligand DTC-BP (**6**), previously used to form a copper-64 complex,[19] in a kit-based approach to synthesise the novel bis(bisphosphonate) complex $^{99m}TcN(DTC\text{-}BP)_2$ ([^{99m}Tc]-**7**) and its rhenium analogues **8** and [^{188}Re]-**8**, and compared their biological behaviour with that of the mono(bisphosphonate) derivative [^{99m}Tc]-**4** and the conventional bone-imaging agent ^{99m}Tc-**1**.

Experimental

Equipment and consumables

TLC analyses were carried out using silica gel on aluminium-backed TLC plates (Merck 1.16834.0001) cut to 100 mm x 25 mm, using four mobile phase systems. Solvent system 1: ethanol/chloroform/toluene/0.5 M ammonium acetate (6/3/3/1);[16] solvent system 2: methanol + 1% of a 60% solution of HEDP (Sigma H6773); solvent system 3: methanol/10% Ammonium Acetate (1/1) containing 15mM EDTA; solvent system 4: 1% HCl in methanol. The spots were allowed to dry before development in the mobile phase. Paper chromatography was carried out using Whatman 3MM paper or Whatman P81 paper and 0.9% saline as mobile phase. Radio-TLC chromatograms were analysed with a Mini-Scan TLC scanner (Bioscan) with FC3600 detector and γ-detector probe and Laura 4.0.2.75 (Lablogic) software. HPLC analyses were carried out on an Agilent 1200 series HPLC with degasser (G1322A), quaternary pump (G1311A), UV detector (G1314B) and manual injector (Rheodyne 7725i). The column used was an Agilent Zorbax Eclipse analytical XDB-C18 column (150 mm x 4.6 mm, 5 µm) unless otherwise indicated. Gamma counting of ^{99m}Tc and ^{188}Re samples was done using a 1282 Compugamma Gamma Counter (LKB Wallac) with Ultroterm software, counting for 10 seconds using a 110-155 KeV window. Higher activities were measured with a CRC-25R (Capintec) dose calibrator. Freeze

drying of samples was done using an Edwards freeze dryer connected to an Edwards RV8 vacuum pump. Mass spectra were acquired on an Agilent 6520 Accurate-Mass Q-TOF LC/MS with electrospray ionisation coupled to an Agilent 1200 HPLC system with degasser, quaternary pump and autosampler (G1329A), using Agilent Masshunter workstation acquisition software, B.02.1 (B2116). Data were analysed using Agilent Masshunter Qualitative software B.03.01 (Build 3.1.346.14 service pack 3). Sample shaking and centrifugation were done on a Grant PHMT shaker and an Eppendorf centrifuge 5424 microcentrifuge, respectively. ^{99m}Tc-**1** (^{99m}Tc-MDP, prepared by reconstitution of a Draximage kit with [^{99m}Tc]-pertechnetate eluted from a generator with physiological saline), was supplied by Guy's Hospital Radiopharmacy, Guy's and St Thomas' NHS trust. [^{188}Re]-perrhenate was eluted with physiological saline from a generator purchased from ITG (Isotope Technologies, Garching GmbH) and, where necessary, concentrated using a previously described procedure.[20, 21] S-methyl-N-methyl-dithiocarbazate (DTCZ) was synthesised as previously described.[22]

Radiolabelling and quality control of [^{99m}Tc]-4

[^{99m}Tc-**4**] was synthesised and characterised according to procedures described previously.[12,23] 50 μg of DPA-ale in 300 μL of 50 mM carbonate buffer (pH 9) containing 0.15 M NaCl was mixed with 300 μL of an aqueous solution of [^{99m}Tc]-$[Tc(CO)_3(H_2O)_3]^+$ (250-300 MBq) in a glass vial with a rubber stopper and heated at 90 °C for 30 min. The product was purified by passing it through a Sep-Pak C-18 Plus Light cartridge (Waters, WAT-23501) activated with absolute ethanol. [^{99m}Tc]-**4** trapped by the column was eluted with 500 μL of 1:1 ethanol:water. The ethanol was then evaporated under a stream of nitrogen and the remaining solution diluted with 250 μL of saline for injection. The intermediates and product were analysed by radio-TLC using solvent system 4 on silica plates (intermediates: reduced hydrolysed technetium, Rf = 0; $[Tc(CO)_3(H_2O)_3]^+$, Rf = 0.1-0.7; pertechnetate, Rf = 0.9; product, [^{99m}Tc-**4**], Rf = 0). Radiochemical purity of the final product was >99%.

Synthesis and mass spectrometry of [TcN(DTC-BP)$_2$] (7)

K[$^{99}TcO_4$] (Amersham International plc, UK; 0.6 mg, 20 μL of a 30 mg/mL solution) was added to a vial containing 3.6 mg succinic dihydrazide (SDH) and 1.3 mg 1,2-diaminopropanetetraacetic acid (DPTA) in 500 μL physiological saline, followed by 500 μL of a 10 mg/mL solution of $SnCl_2$ in 0.05 N HCl. The solution immediately turned yellow/orange and a precipitate formed. After 35 minutes the solution was centrifuged and 50 μL of the supernatant was added to 1.3 mg HDTC-BP (**6**), synthesised as described previously,[19] in 400 μL of pH 10 carbonate buffer. The solution was heated at 60°C for 30 minutes before cooling to room temperature and analysing by mass spectrometry using the LC-MS system without a column. The mobile phase was 15 mM ammonium bicarbonate, adjusted to pH 9.4 with 30% NH_4OH solution. The flow rate was 0.5 mL/min and a splitter was fitted (10% LC flow to mass spectrometer, 90% flow to waste). The mass spectrometer was run in negative ion mode with a gas temperature of 325°C, an N_2 gas flow of 5 L/min and a nebuliser pressure of 20 psi. The capillary voltage was 3500 V and the fragmentor voltages were 175 V and 250 V. The injection volume for each sample was between 0.1 and 1 μL.

Synthesis and mass spectrometry of [ReN(DTC-BP)$_2$] (8).

$[ReNCl_2(PPh_3)_2]$[24] was reacted with 1,3,5-triaza-7-phosphaadamantane (PTA) to produce the water-soluble complex $[ReNCl_2(PTA)_3]$ according to an established method.[25] This complex (8.9 mg, 1.12 x 10^{-5} mol) was dissolved in 1 mL water to give a cloudy brown solution which was then added to **6** (8 mg, 2.46 x 10^{-5} mol, 2.2 eq) and shaken at 800 rpm at room temperature for 80 min. The solution was then freeze dried. The freeze dried material was reconstituted to 1 mg/mL in water for mass spectrometry analysis, giving a clear yellow solution. This was analysed by mass spectrometry as described above for [^{99}Tc]-**7** but with fragmentor voltage set at 125 V or 325 V.

Radiolabelling of [^{99m}Tc]-7

Method 1 (arrived at after extensive optimisation to ensure reliable quantitative radiochemical yield): To a vial containing SDH (2.5 mg) and DPTA (1 mg) in 500 μL saline was added 695 MBq $^{99m}TcO_4^-$ generator eluate (120 μL), followed by 50 μL of a 10 mg/mL solution of $SnCl_2$ in 0.05 N HCl. The mixture was shaken at room temperature for 1 h. Quality control was performed using TLC with solvent system 1 (pertechnetate, Rf = 0.5; reduced hydrolysed technetium, Rf = 0; required technetium nitride intermediate, Rf = 0 – 0.3) and solvent system 2 (reduced hydrolysed technetium, Rf = 0; required technetium nitride intermediate and pertechnetate, Rf = 0.9). 300 μL of this solution was then added to a vial containing 0.5 mg **6** in 200 μL carbonate buffer, to give a total of 280 MBq in 500 μL. The solution was heated at 60°C for 30 minutes, followed by quality control by TLC using solvent system 2 ([^{99m}Tc]-**7**, Rf = 0). For *in vivo* administration 200 μL of the solution was added to 80 μL 0.1 N HCl, to give 101 MBq of ^{99m}Tc-**7** in 280 μL with a final pH of 6.6-7.

Method 2 (developed after optimising the synthesis via method 1): 623 MBq $^{99m}TcO_4^-$ generator eluate (in 1 mL saline) was added to a lyophilised SDH kit vial (generous gift of Prof. Roberto Pasqualini, Cis Biointernational, IBA Group, Gif-sur-Yvette, France,

as previously used for production of ^{99m}Tc-NOET)[17, 18] and incubated for 30 minutes at room temperature. The composition of the kit vial was as follows: SDH 5.0 mg; stannous dichloride dihydrate 0.10 mg; DPTA 5.0 mg; sodium dihydrogen phosphate monohydrate 0.6 mg; disodium phosphate heptahydrate 10.9 mg; under a dinitrogen atmosphere. Quality control was performed using TLC with solvent system 1. 300 µL of the resulting solution was then added to 300 µL of the of DTC-BP ligand (1 mg/mL) in carbonate buffer (pH 10). The vial was incubated at 60 °C for 30 minutes. QC was performed using TLC with solvent system 2.

Radiolabelling of [^{188}Re]-8

Kit vials were prepared as follows: 1.5 mg DTCZ was placed in a nitrogen-purged vial followed by 2.8 mg/mL $SnCl_2.2H_2O$ dissolved in 0.5 mL of 20 % glacial acetic acid and 28 mg sodium oxalate. The vial was capped with a rubber stopper, sonicated and purged with nitrogen for 10 min. To a kit vial thus prepared, 500 MBq $^{188}ReO_4^-$ in 0.5 mL generator eluate was added. The vial was vortex-mixed, heated at 80°C for 2-3 min and allowed to cool to room temperature for 15 min. TLC was performed using solvent system 1 above. This intermediate solution as also analysed by radioHPLC using an Agilent HPLC with an Eclipse XDB-C18 column (4.6 x 150 mm) and a guard column eluted with 95% water, 5% methanol each with 0.1% trifluoracetic acid, at a flow rate of 1 mL/min. In this system perrhenate (5% of eluted activity) eluted at < 2 min, while the rhenium nitride intermediates (95% of eluted activity) eluted as a series of isomeric species at 10-13 min. 50 µL of this solution of ^{188}Re-nitride intermediate was then added to 71.4 µg DTC-BP in 100 µL carbonate buffer (0.5 M, pH 9.0), to give a total of 25 MBq in 150 µL. The solution was gently vortexed and heated at 80°C for 30 min, followed by quality control by TLC using solvent system 3 (perrhenate, Rf = 0.8-0.9; [^{188}Re]-**8**, Rf = 0).

LogP measurement

The lipophilicity of each ^{99m}Tc and ^{188}Re radiotracer, with a radiochemical purity of at least 95%, was determined by partitioning the complex between 1-octanol and water. 50 µl (~1-2 MBq) of the radiotracer was added to a 1.5 mL Eppendorf tube (n = 9) containing 500 µL 1-octanol and 495 µL of distilled water and vortexed at room temperature for 15 minutes and then centrifuged at 1200 RPM for 5 minutes. A 0.2 mL aliquot of each phase was pipetted out and counted in a gamma-counter. The partition coefficient was calculated as logP = log((cpm in octanol–cpm background)/(cpm in water–cpm background)).

Synthetic and biological mineral binding studies

Preparation of mineral salts and buffer solutions: 1 mg of each bone mineral analogue (hydroxyapatite, β-tricalcium phosphate, calcium phosphate dibasic, calcium oxalate, calcium carbonate or calcium pyrophosphate, all purchased from Sigma-Aldrich) was added to a 1.5 mL plastic microcentrifuge tube in duplicate. 1 mL TRIS-HCl buffer (50 mM, pH 6.8) was added to each tube followed by 10 µL of either ^{99m}Tc-**7** (prepared by method 1) or 10 µL of the $^{99m}TcN^{2+}$ intermediate (method 1, as a control). 10 µL of either tracer were also added to control tubes containing 1 mL TRIS-HCl with no mineral salts. All tubes were then shaken at 900 rpm for 1 h then centrifuged at 10,000 rpm for 5 min. 10 µL of supernatant was removed from each tube (including the controls) and added to 1 mL TRIS-HCl buffer (50 mM, pH 6.8) in triplicate. Percentage binding of radioactivity to the mineral salts was calculated as $(1 - cpm_{sample}/cpm_{control}) \times 100\%$.

Similar studies were performed with mineral samples of biological origin, including powdered equine bone and human minerals isolated from vascular intimal and medial calcified plaques obtained from surgical procedure with appropriate ethical approval. The methods to release these biominerals from their organic matrix and connective tissues have been previously published.[26, 27] Suspensions of 0.5 mg/mL of each sample were prepared in distilled water. 1 mL of the suspensions in triplicate (synthetic hydroxyapatite, powdered equine bone, medial and intimal arterial minerals) was placed in 1.5 mL Eppendorf tubes in triplicate alongside mineral-free controls. 20 µL of ^{99m}Tc-**1**, [^{99m}Tc]-**4** and [^{99m}Tc]-**7** (0.5-1 MBq) was added to each tube. The tubes were incubated for 60 min in a shaker at 37 °C and 550 RPM. The tubes were centrifuged at 13,200 RPM for 5 minutes. 50 µL of the supernatant from the vials were pipetted out and counts were measured in a gamma counter. The binding percentage was calculated as above.

Hydroxyapatite binding in the presence of serum and serum protein binding

To microcentrifuge tubes containing 2 mg/mL hydroxyapatite in TRIS-HCl buffer (50 mM, pH 6.8) or human serum (Sigma) were added 10 µL of either [^{99m}Tc]-**7** or ^{99m}Tc-**1**. Identical controls without mineral were prepared similarly. All tubes were prepared in triplicate. All samples were then incubated with shaking at 1400 rpm at 37°C. At intervals of up to 23 h all tubes were centrifuged at 10,000 rpm for 5 minutes. 5 µL supernatant was removed from each tube and counted in a gamma counter. Hydroxyapatite % binding was calculated as described above. Binding to serum proteins in the serum-containing samples was assessed as follows: 70 µL ethanol was added to 50 µL aliquots of the supernatant after centrifugation of each serum incubation. The tubes were centrifuged at 10,000 rpm for 5 minutes and the supernatant was removed. The pellets were washed with another 70 µL ethanol,

centrifuged again and the supernatant was decanted and added to the supernatant from the initial precipitation. The pellets and supernatant were then counted separately in a gamma counter. Percentage serum protein binding was calculated as 100% x $cpm_{pellet}/(cpm_{pellet}+cpm_{supernatant})$. Control samples of [^{99m}Tc]-**7** in buffer were also subjected to ethanol precipitation to ascertain whether or not the addition of ethanol caused the complex to precipitate.

Animal studies

All procedures were performed in accordance with licences and guidelines approved by the UK Home Office and were approved by a King's College ethics committee. Normal female BALB mice, 9 weeks old, were used for preliminary comparative biodistribution studies with ^{99m}Tc-**1**, [^{99m}Tc]-**7** and [^{188}Re]-**8**. For imaging of arterial calcification, Sprague Dawley rats (n = 6; male; 21-27 days old) were purchased from Charles River Laboratories. After an acclimatisation period of 7 days, 6 rats were fed with a diet containing warfarin (3 mg/g food) and vitamin K1 (1.5 mg/g food) for 11 days. The rats were given 200,000 IU/kg/day subcutaneous injections of cholecalciferol (Sigma- 47763) from day 7 to day 11 of the diet. It has been reported that warfarin treatment in the form of diet, oral administration (gavage) or subcutaneous injections induces vascular calcification[27, 28] and the process is accelerated by vitamin D_3 (cholecalciferol). All animals were maintained on a 12 hour light-dark cycling with access to environmental enrichment (tunnel). Food and water were provided *ad libitum*.

SPECT/CT scanning and biodistribution: Mice (n=1) under Isoflurane anaesthesia were injected with 40 MBq of either [^{99m}Tc]-**1** or [^{99m}Tc]-**7** in ~ 100 µL via a tail vein. SPECT-CT scans were acquired at intervals up to 338 min using a NanoSPECT-CT scanner (Bioscan, USA) with SPECT acquisition time 1800 s, obtained in 24 projections using a 4-head scanner with 4 × 9 (2 mm) pinhole collimators in helical scanning mode and CT images with a 45 kVP X-ray source, 500 ms exposure time in 180º projections over 9 min. Images were reconstructed in a 128 × 128 matrix using HiSPECT (ScivisGmbH), a reconstruction software package, and images were fused using proprietary Bioscan InVivoScope (IVS) software. All scans were 30 minutes long. Kinetic studies (% uptake) were carried out by calculating the radioactivity in local regions of interest (ROIs) relative to the radioactivity in the whole body ROI. ROI data were calculated for both a knee joint and a single vertebra. The mice were sacrificed with an overdose of anaesthesia at the end of scanning and the organs and tissues were harvested, weighed and counted in a gamma counter. Uptake was reported as standard uptake values (SUVs). Rats under Isoflurane anaesthesia were injected with 40-50 MBq (100 µL) of the radiotracers via a tail vein with ^{99m}Tc-**1**, [^{99m}Tc]-**4** or [^{99m}Tc]-**7** (n = 2 in each case). CT images were acquired with a 55 kVP X-ray source, 100 ms exposure time in 360º projections over 24 min. SPECT imaging was performed with above mentioned parameters at intervals of 30 min up to 240 min. After 4 hours of SPECT-CT scanning the rats were culled by an overdose of anaesthesia. Vital organs were harvested, weighed and counted with a gamma counter, along with standards prepared from a sample of the injected material. The percent of injected dose per gram of tissue (% ID/g) was calculated. Biodistribution of [^{188}Re]-**8** was determined similarly (n = 3) after injection of 8.5 MBq (50 µL) of the radiopharmaceutical. Mice were killed at 24 h post-injection and organs harvested as described above, weighed and counted in a gamma counter.

Figure 2: Intermediates and products (the latter as identified by detection of corresponding molecular ions in electrospray mass spectrometry) in the synthesis of rhenium nitride complexes.

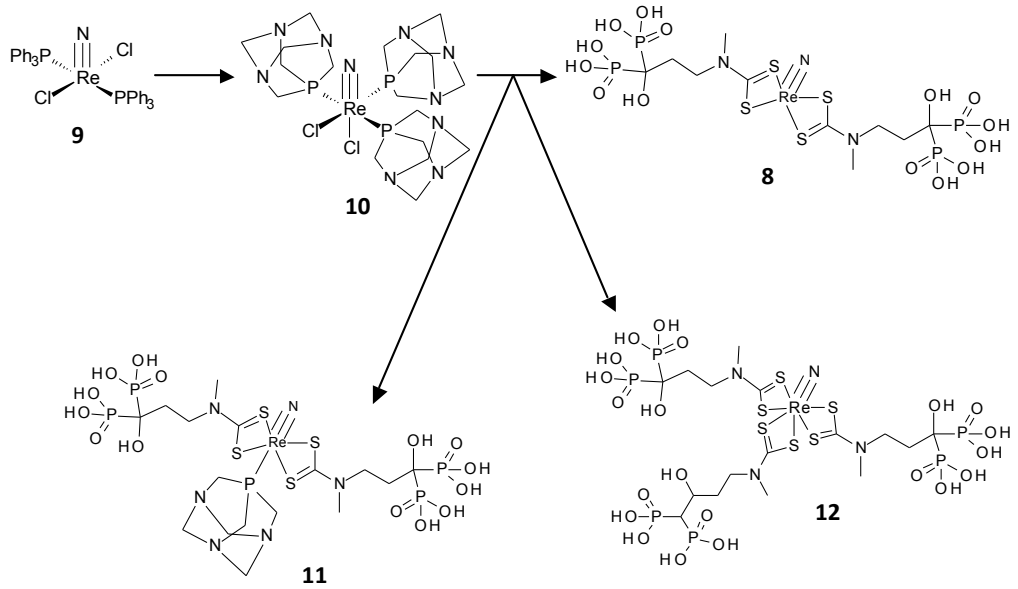

Figure 3: Radio-TLC chromatograms on silica gel coated aluminium plates of (A) $^{99m}TcO_4^-$, solvent system 1; (B) $^{99m}TcN^{2+}$ intermediate, solvent system 1, (demonstrating the absence of pertechnetate at this stage); (C) $^{99m}TcN^{2+}$ intermediate, solvent system 2 and (D) ^{99m}Tc-**7**, solvent system 2 (demonstrating the absence of both pertechnetate and the Tc-nitride intermediate in the final product).

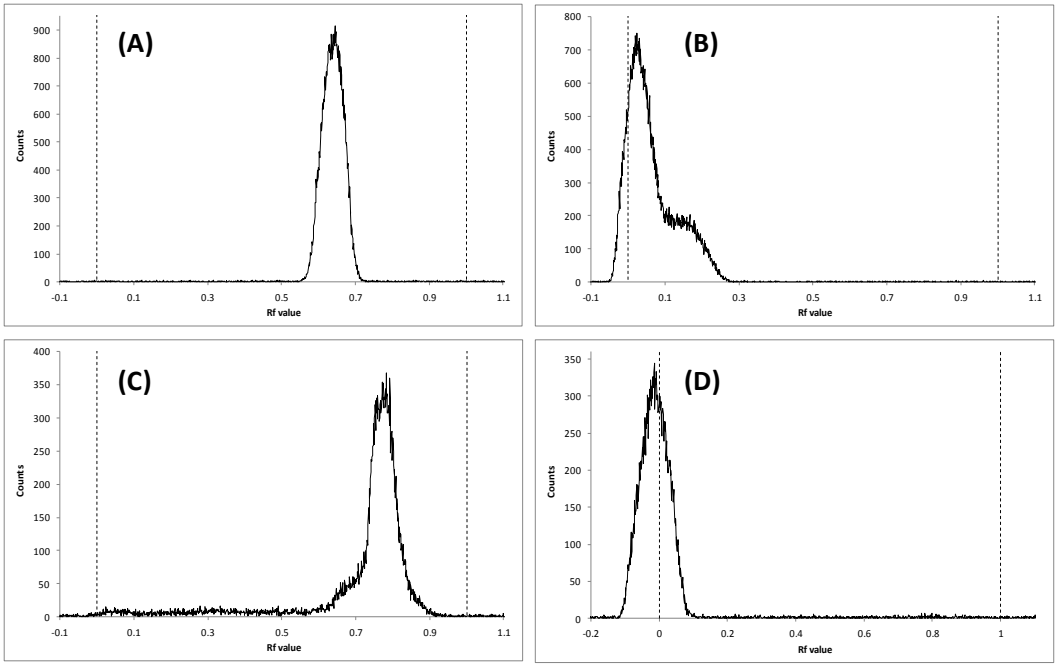

Results

Chemical syntheses and characterisation

[TcN(DTC-BP)$_2$] (7): The beta-emitting isotope ^{99}Tc has a long half-life (200,000 years) and hence, unlike the gamma-emitter ^{99m}Tc, a low enough specific activity to be handled in quantities sufficient to perform conventional spectrometry. Compound **8** was synthesised by a scaled-up version of the no-carrier-added method used with ^{99m}Tc (see below), starting from potassium pertechnetate and reducing it with stannous chloride in the presence of succinic dihydrazide as a nitride source and propane-1,2-diamine tetraacetic acid as an intermediate chelator of the technetium complex and possibly of tin. Like the rhenium analogue (see below for details), the clear yellow solution resisted isolation of the product in pure form by virtue of its intractable solubility and chromatography properties, and was therefore characterised by electrospray mass spectrometry (again, like the rhenium analogue discussed below). Negative ion mass spectra of the yellow ^{99}Tc solution show that at 250 V the only technetium-containing ions detected were those derived from the expected molecule **7** i.e. $(M-H)^-$ (*m/z* = 759.8003) and sodium adducts $(M-2H+Na)^-$ (781.7815) and $(M-3H+2Na)^-$ (803.7624). At 175 V the doubly charged $(M-2H)^{2-}$ species was also present. No ions containing Tc in a form other than this (e.g. with oxo-ligand rather than nitride, or with a ligand-to-metal ratio other than 2:1, or oligomeric species) were detected. A full list of ions can be found in table S2 of the supplementary data, along with raw spectra.

[ReN(DTC-BP)$_2$] (8): Synthesis of **8** was achieved in three steps. The well-known Re(V) nitride precursor $[ReNCl_2(PPh_3)_2]$ was synthesised according to an established method[24] and was then reacted with 1,3,5-triaza-7-phosphaadamantane (PTA) to make the water-soluble $[ReNCl_2(PTA)_3]$ according to an established method.[25] The aqueous solubility of $[ReNCl_2(PTA)_3]$ enabled its reaction with the dithiocarbamate-bisphosphonate conjugate **5** which is soluble only in water; the resulting clear yellow aqueous solution was typical in appearance to previously reported $[ReN(dtc)_2]$ complexes but because of the extreme water solubility of the product, its extreme insolubility in non-aqueous solvents, and its strong adherence to all of the wide variety of chromatographic stationary phases tested (including reverse-phase silica-based HPLC media) it remained resistant to isolation in pure form. Therefore the crude clear yellow aqueous solution was analysed by electrospray mass spectroscopy (in negative mode due to the expected negative charge), as the only analytical approach by which the complex could be characterised without interference from other components of the mixture. Because of the irreversible adsorption to all chromatographic media, the LC-MS system was used without a column. The sample was analysed at two different cone voltages. At 325 V the only ion species showing the characteristic $^{185/187}$Re isotope pattern were the negatively charged ions corresponding to the expected molecule **8** ionising by loss of H^+ or $2H^+$, and variants with H^+ replaced by Na^+. In the case of the dominant ^{187}Re isotope these were $(M-H)^-$ complex (*m/z* = 847.8721) and related sodium

adducts $(M\text{-}2H+Na)^-$ (869.8517) and $(M\text{-}3H+2Na)^-$ (891.8341), and doubly charged relatives $(M\text{-}2H)^{2-}$ (*m/z* = 423.4129) and related sodium adducts $(M\text{-}3H+Na)^{2-}$ (434.4033) and $(M\text{-}4H+2Na)^{2-}$ (445.3949). The mass spectrum also showed another ^{187}Re species with *m/z* 765.8919 (together with its ^{185}Re partner), corresponding to a fragmentation involving loss of $P(OH)_3$ and ionisation by loss of H^+. No ions of higher molecular weight that would indicate oligomeric species, or with ratios of ligand-to-rhenium nitride other than 2:1, or indeed rhenium species not containing the nitride ligand, were detected in the mass spectrum at 325 V. At 125 V, the main species identified were again the doubly charged $(M\text{-}2H)^{2-}$ derived from **8** and related sodium adducts $(M\text{-}3H+Na)^{2-}$ and $(M\text{-}4H+2Na)^{2-}$. However, also present at 125 V were peaks derived from [ReN(DTC-BP)$_2$(PTA)] with $(M\text{-}H)^-$ and $(M\text{-}2H)^{2-}$ and related sodium adducts. There was also a set of peaks relating to ReN(DTC-BP)$_3$ (M-H). The absence of these peaks from the 325 V spectrum of the same sample suggests that they appear of greater significance under the milder ionisation conditions because the major species derived from **8** itself are less efficiently ionised at this low voltage. A full list of ions can be found in table S1 of the supplementary data along with the raw spectra.

Radiolabelling and quality control of [^{99m}Tc]-7

The radiolabelling method was developed from the established two-step methods used for radiolabelling the lipophilic ^{99m}TcN(DTC)$_2$ complexes such as ^{99m}Tc-NOET.[15-17] The general method was to make the pentavalent $^{99m}TcN^{2+}$ intermediate (presumably with PDTA as ancillary ligands) from pertechnetate by stannous reduction in the presence of succinic dihydrazide as the nitride source in the first step before adding this solution to the dithiocarbamate (in this case **5**) in the second step. As expected from the adsorption and solubility behaviour of **8** (above), analysis of radiochemical purity of [^{99m}Tc]-**7** using reverse phase HPLC proved to be unsuccessful, leading to retention of all radioactivity on all columns evaluated (whether reverse- or normal-phase) even after prolonged washing with various solvents. The nitride intermediate and the starting pertechnetate were, on the other hand, eluted successfully from HPLC columns and migrated in suitable TLC conditions, as expected. Two solvent systems were adopted for quality control using silica gel TLC. Solvent system 1 could distinguish between $^{99m}TcO_4^-$ and the $^{99m}TcN^{2+}$ intermediate (Figure 3, A and B respectively). Solvent system 2 could distinguish between the $^{99m}TcN^{2+}$ intermediate and [^{99m}Tc-**7**] (Figure 3, C and D respectively); all three species could be distinguished using these two systems. Thus, the main evidence for the formation of the required [^{99m}Tc]-**7** is the presence of a radioactive species with Rf = 0 under conditions of both TLC methods 1 and 2; no such species appeared at earlier stages of the synthesis. These TLC methods were used to optimise the kit-based process for synthesising [^{99m}Tc]-**7**, before finally arriving at the conditions described in the experimental section. Octanol-water solvent extraction confirm that [^{99m}Tc]-**7** is highly hydrophilic (logP = -2.76 ± 0.08), and its increased lipophilicity compared to ^{99m}Tc-**1** and [^{99m}Tc]-**4** (logP = -2.40 ± 0.16 and 2.05 ± 0.03 respectively; see supplemental information) is consistent with the presence of two pendant bisphosphonate groups.

Radiolabelling and quality control of [^{188}Re]-8

The approach to ^{188}Re radiolabelling was similar to that used for ^{99m}Tc labelling. First a labelled rhenium-nitrido intermediate was prepared using stannous chloride to reduce rhenium from Re(VII) to Re(V) and DTCZ as a source of the nitride group, as previously described.[29] TLC and HPLC showed that at this stage 95% of perrhenate had been converted to the intermediate. This intermediate was then treated with the dithiocarbamate ligand to produce [^{188}Re]-**8**, which was used both to confirm the equivalence of the radioactive species by TLC with the cold complex characterised by mass spectrometry, and for preliminary biodistribution studies. The final TLC showed that no perrhenate or intermediate remained in the product. As in the case of [^{99m}Tc]-**7**, no HPLC or TLC conditions could be found in which the product could be eluted from the stationary phase.

Figure 4 Graph showing results of bone mineral binding studies of [^{99m}Tc]-**7** (hatched bars) and $^{99m}TcN^{2+}$ intermediate (black bars).

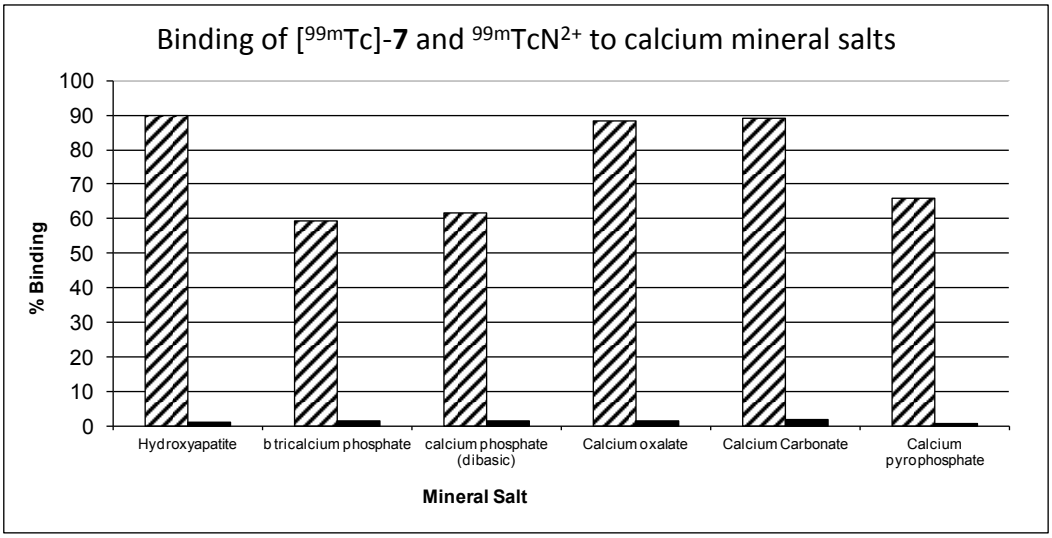

***In vitro* bone mineral binding studies**

To determine the propensity of the complexes to bind to hydroxyapatite (HA) and other calcium phosphates, as a crude *in vitro* assessment of bone targeting potential and to confirm the availability of bisphosphonate groups for mineral binding, [^{99m}Tc]-**7** was mixed with a suspension of hydroxyapatite and allowed to partition between solid and solution phase. Binding of [^{99m}Tc]-**7** was high for each mineral salt with values ranging between 59% for β-tricalcium phosphate up to 90% for hydroxyapatite as shown in figure 4. "Non-specific" binding of radioactivity of the $^{99m}TcN^{2+}$ intermediate to mineral salts was very low with all values ≤ 1.6%. This encouraging result prompted comparison of [^{99m}Tc]-**7** with the other ^{99m}Tc-bisphosphonate complexes, ^{99m}Tc-**1** and [^{99m}Tc]-**4**, in their affinity for synthetic and biologically-derived calcium phosphates.

Each of these ^{99m}Tc-complexes was incubated with 0.5 mg/mL of synthetic HA, equine bone and isolated minerals from human intimal and medial atherosclerotic plaque samples. The results are shown in figure 5. The percentages of ^{99m}Tc-**1**, [^{99m}Tc]-**4** and [^{99m}Tc]-**7** bound to synthetic HA were 88.5±0.9%, 92.4±0.7% and 94.5±3.05% respectively. A similar range and ranking was observed with powdered bone and with mineral from medial calcified plaques. However with the minerals isolated from intimal plaques the % binding was significantly lower (possibly because these minerals contain a lipid component) and the MDP complex had a markedly reduced tendency to bind compared to the pendant bisphosphonate complexes.

Figure 5: Graph showing the % binding (mean ±SD) of ^{99m}Tc-**1**, [^{99m}Tc]-**4** and [^{99m}Tc]-**7** with synthetic hydroxyapatite, powdered equine bone and minerals from intimal and medial plaques. *significant a p>0.05, **significant at p>0.001 and ***significant at p>0.0001.

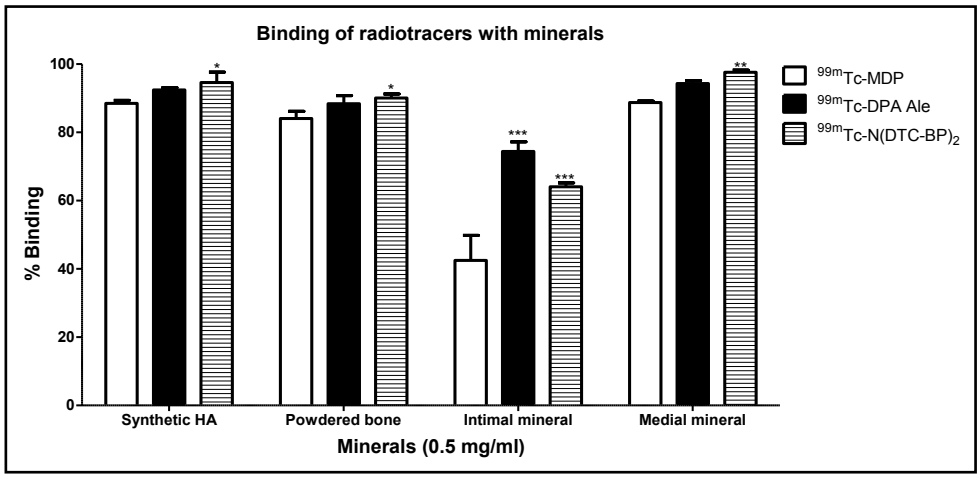

Binding to hydroxyapatite and proteins in serum

^{99m}Tc-**1** and [^{99m}Tc]-**7** were incubated in serum (and a non-phosphate buffer, as a control) with and without hydroxyapatite over a period of 23 h in order to determine whether a biological milieu interferes with mineral binding, and to compare their binding to serum proteins. [^{99m}Tc]-**7** binds well (>90%) to hydroxyapatite in buffer and only slightly less well (>80%) in serum, and the binding is largely retained during the 23 h. ^{99m}Tc-**1** on the other hand binds less well in buffer (>60%) in qualitative agreement with figure 6 despite the changed conditions, and the binding is severely diminished (>30%) by the presence of serum; moreover the fraction bound in buffer diminishes with time (to *ca.* 35% by 23 h), whereas there is no corresponding loss of binding with time in serum. Possibly this behaviour is associated with vulnerability of ^{99m}Tc-**1** to gradual oxidation to pertechnetate, against which serum may offer some protection, and to which [^{99m}Tc]-**7** is less sensitive because of the more appropriately designed chelator used. Both complexes display a high level of binding to proteins (70-80% in the case of [^{99m}Tc]-**7**, 60-70% in the case of ^{99m}Tc-**1**), with a much faster loss of protein binding over time in the case of ^{99m}Tc-**1**, possibly again because of gradual oxidation to pertechnetate.

Figure 6: Graph showing binding of [^{99m}Tc]-**7** to hydroxyapatite in buffer (black solid line) and in serum (black dotted line); ^{99m}Tc-MDP in buffer (grey solid line) and in serum (grey dotted line).

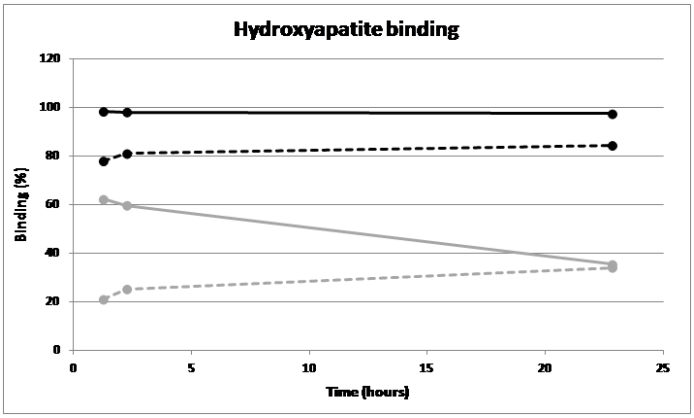

Biodistribution and imaging

The biodistribution of the new tracer [^{99m}Tc]-**7** was compared with that of the conventional bone imaging agent ^{99m}Tc-**1** in normal mice. Both tracers (figure 7) show qualitatively similar biodistribution, with high uptake in bone and especially the joints, no marked uptake in any other tissue except kidney and bladder but a marked difference in the rate at which the tracer accumulates and clears through the renal pathway. The biodistribution of ^{99m}Tc-**1** reached a steady state by 100 min, with renal excretion essentially complete and no further uptake in or clearance from bone and joints. [^{99m}Tc]-**7** on the other hand was still visibly being excreted through kidney at this time, while figure 8 shows that activity continued to migrate from blood and soft tissues to bone and joints until at least 6 h. Although the SUV of [^{99m}Tc]-**7** in bones and joints was lower than that of ^{99m}Tc-**1** at 1 h, by 2 h the

SUVs were similar and by 6 h the SUV of [^{99m}Tc]-**7** was significantly higher than that of ^{99m}Tc-**1**. The bladder (removed from the image for clarity of display) contained 61% of the radioactivity from 104 minutes onwards for ^{99m}Tc-**1** compared with 24% at 54 minutes for [^{99m}Tc[-**7**, rising to 28% at 365 minutes post injection.

Figure 7: SPECT images (coronal sections) of a mouse injected with [^{99m}Tc]-**7** at 54 min (A) and 365 min (B), and of a mouse injected with ^{99m}Tc-**1** after 104 min (C) and 368 min (D), post injection. The bladders have been digitally removed from the field of view for the sake of clarity. All scans show high uptake in bone and especially joints. A and B show transit and retention of activity by kidney, whereas in C and D the renal excretion process is essentially complete and the kidneys are not evident.

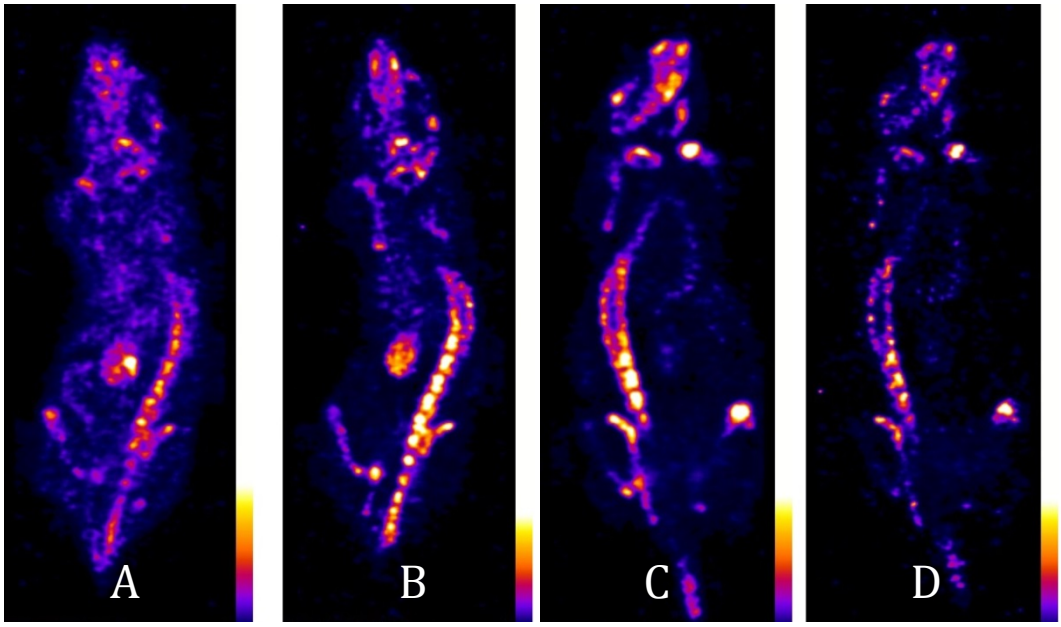

Biodistribution data at 6 h post injection are shown in Fig. 9. SUVs are higher in bone and joint for [^{99m}Tc]-**7** compared with ^{99m}Tc-**1** but non-specific binding in most soft tissues is higher for [^{99m}Tc]-**7** particularly in the kidneys because of slower excretion and slower binding to bone, and minor uptake in trachea, spleen and liver. Also of note from figure 8 is that [^{99m}Tc]-**7** displays a higher ratio of uptake in joint to mature bone than ^{99m}Tc-**1**.

Figure 8: Graph showing uptake in knee joint (solid lines) and single vertebra (broken lines) over 6 h. ^{99m}Tc-**7** is represented by black lines, ^{99m}Tc-**1** is represented by grey lines.

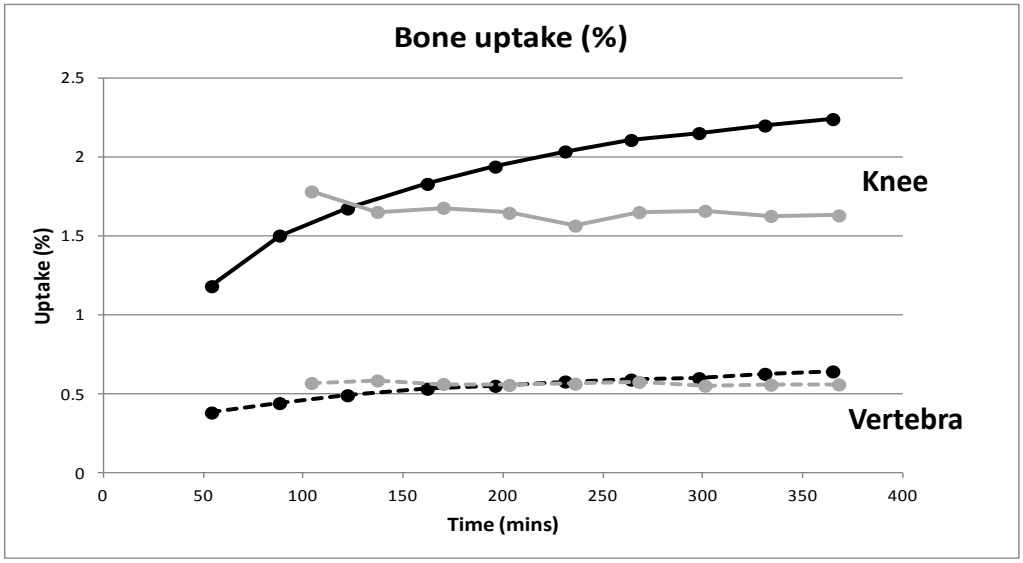

Figure 9: Standard Uptake Values (SUVs) for ^{99m}Tc-**1** (grey bars) and [^{99m}Tc]-**7** (black bars) in mice at 6 h post injection.

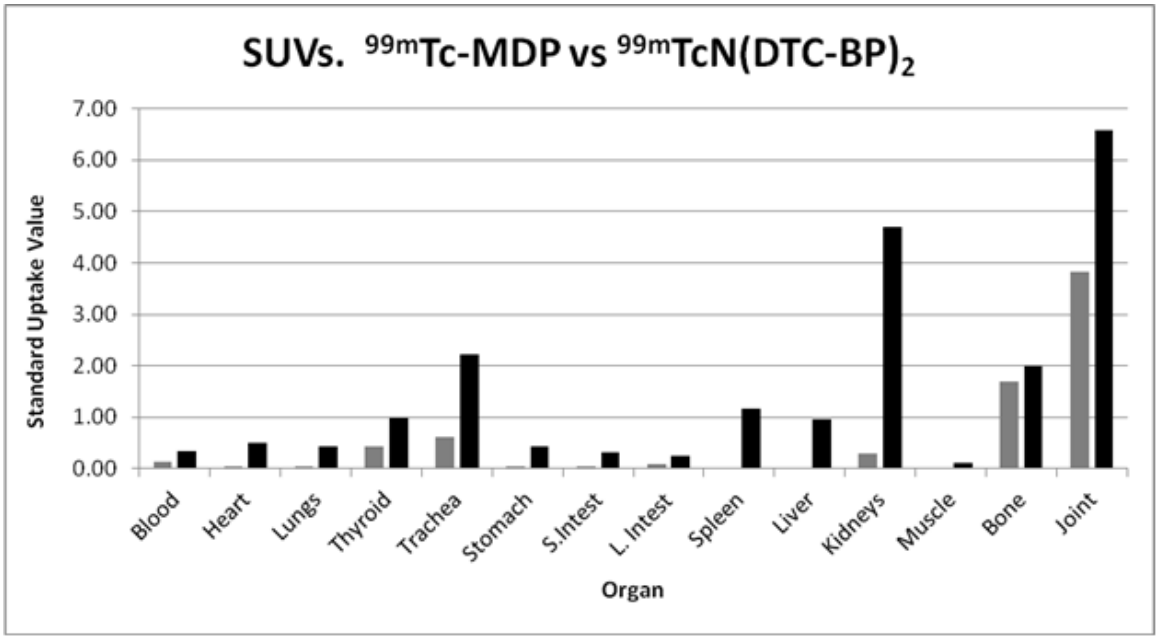

The new rhenium-188 radiopharmaceutical [^{188}Re]-**8**, like [^{99m}Tc]-**7**, shows high specificity for bone and joints in preliminary biodistribution studies in mice (see supplemental information). Radioactivity concentration in bone and joints is high at 24 h (a much later time point than in the evaluation of its ^{99m}Tc analogue) and higher than in kidney and other tissues.

The ability of the tracers to detect vascular calcification was compared in a rat model in which arterial calcification was induced by administration of warfarin and vitamin K in the diet and vitamin D subcutaneously. The resulting arterial calcification in the aorta and mesenteric arteries was confirmed by histological staining (see supplemental information). SPECT-CT scans (figure 10 and supplemental information) were then performed with novel agents [^{99m}Tc]-**7** and [^{99m}Tc]-**4** and the conventional agent ^{99m}Tc-**1**. As well as in bones and joints, intense uptake of all the radiotracers was most strikingly seen in the calcified mesenteric artery within 30 min of the injection. This manifests as a hollow sphere of activity, in the abdominal region below the liver that does not correspond to any major solid organs and is not visible in scans of normal rats. *Ex-vivo* biodistribution demonstrates significantly increased uptake (%ID/g) in most tissues (including bones) compared to normal rats; of the tissues that could be dissected and weighed (which do not include the mesenteric arteries), the increase is particularly marked for all three tracers in the aorta, heart and lungs (figure 11) although uptake in these organs is still too small to be clearly evident on the scans at the thresholds used in figure 10. While these data demonstrate the ability of the new tracers to detect vascular calcification, at the present stage of analysis they do not demonstrate any dramatic advantage in sensitivity of the new tracers with pendant bisphosphonate groups compared to the conventional heterogeneous tracer ^{99m}Tc-**1** in this application.

Discussion

We have described a simple synthesis and radiolabelling of the first technetium and rhenium complexes with two pendant bisphosphonate groups, building on the early development of complexes in which bisphosphonate groups are bound directly to the radiometal (and which have become established radiopharmaceuticals for imaging and palliative therapy of bone disease[2]) and the later development of complexes containing a pendant bisphosphonate group.[12, 13] We reasoned that this sequence of developments in design should yield radiopharmaceuticals with improved homogeneity, *in vivo* stability and targeting of biomineral deposits. To produce a well-defined complex with two pendant bisphosphonate groups we chose to use the well-known technetium/rhenium(V) nitridobisdithiocarbamate core, in conjunction with a dithiocarbamate-bisphosphonate conjugate ligand, **6**, which we previously showed to coordinate to copper(II) via its dithiocarbamate group to form a complex with two pendant bisphosphonate groups.[19]

Figure 10: A, B: Coronal sections of a rat scanned 30 min and 4 h, respectively after i.v. injection of [^{99m}Tc]-**7**. C, D: Coronal sections of a rat scanned at 30 min and 4 h, respectively, after i.v. injection of [^{99m}Tc]-**4**. E, F: Coronal sections of a rat scanned at 30 min and 4 h, respectively, after i.v. injection of ^{99m}Tc-**1**. Arrows show the uptake of the radiotracers in the calcified mesenteric arteries.

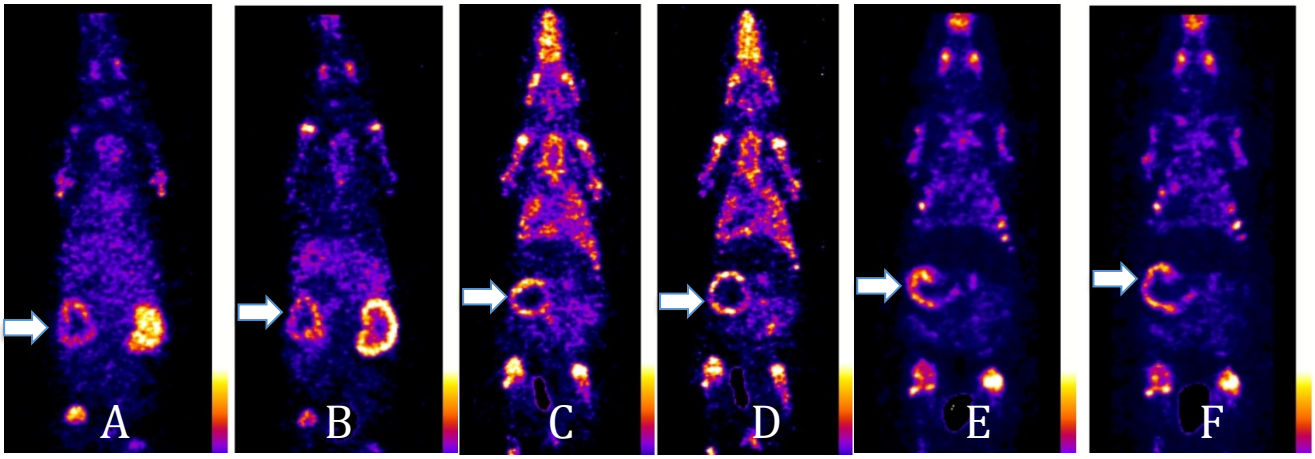

The synthesis of the ^{99}Tc and ^{99m}Tc complexes is based on the established formation of a M(V) nitride complex using succinic dihydrazide as a source of nitrogen to form the nitride.[17, 18] To establish a robust, kit-based synthesis with sufficiently high yield (>95%) to avoid the need for a purification step, it was necessary to optimise the composition of the kit and in particular to ensure that the concentrations and molar ratios of the intermediate chelator DPTA and the final ligand **6** were appropriately balanced: too little DPTA leads to inadequate stabilisation of the metal nitride intermediate, while too much causes competition with the dithiocarbamate ligand in the second step. This optimisation led to methods 1 and 2 each of which provides a simple route to the ^{99m}Tc complex. The ^{99}Tc analogue was also synthesised, using the same reagents, to generate sufficiently high concentrations for analysis by mass spectrometry. The route to the rhenium complex was based on conventional rhenium nitride starting materials, adapted for compatibility with an aqueous synthesis because **6** is only soluble in water.

The characterisation of the product complexes posed major problems because the solubility and adsorption properties of both **7** and **8** precluded purification by recrystallisation or chromatography. The bisphosphonate complexes are all extremely hydrophilic (see logP data, supplemental information) and adherent to various stationary phases. As a result, only negative ion electrospray mass spectrometric data are available to confirm the identity of the products. The mass spectra, however, confirm several key aspects relating to the structure and homogeneity of both **7** and **8**. The ions observed are consistent with the presence of a mononuclear nitrido complex with two dithiocarbamate-bisphosphonate ligands, with the metal in oxidation state five. This is consistent with the body of literature on technetium and rhenium nitride bis(dithiocarbamate) complexes.[14] These data cannot, however confirm that ligand is coordinated through the dithiocarbamate group rather than the bisphosphonate group; but comparison with literature on technetium and rhenium with coordinated bisphosphonates would suggest such complexes are inhomogenous and polymeric,[8, 9] and there is no evidence of such behaviour in the mass spectra of **7** and **8**. Moreover, dithiocarbamates are well known to form transition metal complexes with high affinity, whereas bisphosphonates and pyrophosphates are have been used because of their relative instability, as intermediate chelators to make metastable Tc intermediates in which the bisphosphonates are ultimately displaced by more powerful ligands (e.g. during protein radiolabelling at thiol groups of reduced antibodies[30]). The mass spectra are also unable to distinguish possible isomers due to the different relative orientations of the ligands (e.g. *syn*- and *anti*- disposition of the methyl groups of the two ligands); however, this is unlikely to be problematic because the metal coordination sphere in this class of complexes is well-known to be highly fluxional. The equivalence of carrier free (radiolabelled, characterised only by virtue of its Rf value of zero on TLC) and carrier added ($^{185/187}$Re and ^{99}Tc, identified by mass spectrometry and Rf value of zero on TLC) is demonstrated only by sharing Rf values of zero in various TLC conditions and failure to elute from various HPLC columns. This is weak evidence because many species such as reduced hydrolysed Tc share this property. However, although differences in structure and speciation of radioactivity are often observed in technetium complexes at the tracer an macroscopic levels, these typically involve oligomerisation at the higher concentration but not at the lower; since the high concentration solutions here have been shown by mass spectrometry to contain only mononuclear complexes, there is no reason to doubt that the tracer level complexes are also mononuclear.

Figure 11: Biodistribution (%ID/g, mean±SD) in rats 4 h after injection of tracers ^{99m}Tc-**1**, [^{99m}Tc]-**4** and [^{99m}Tc]-**7** (n=2).

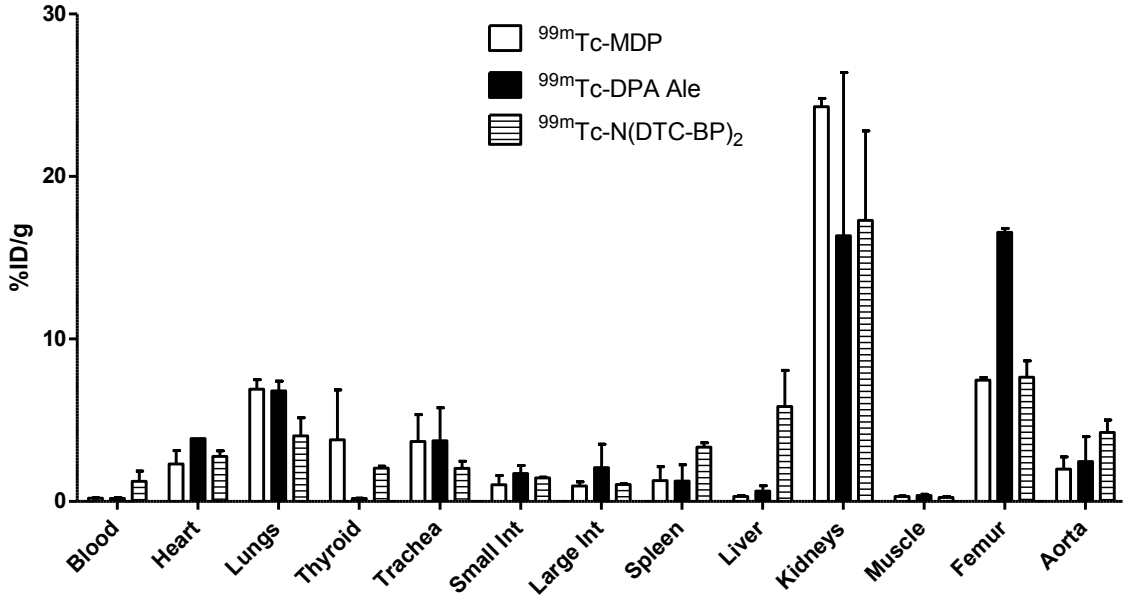

Both the new pendant tracers [^{99m}Tc]-**4** and [^{99m}Tc]-**7** show improved binding both to synthetic calcium-based minerals and to hydroxyapatite-like minerals isolated from human calcified tissue, and improved stability in buffer and serum compared to ^{99m}Tc-**1**, as indeed they were designed to do. This advantage is conferred by the design of the metal coordinating ligands to match the known preferences of the metal core, rather than relying on the relatively poor chelating ability of the bisphosphonate group. This translates into improved stability in buffer and blood serum, and *in vivo*, which in turn leads to higher uptake in bone and calcified soft tissues than ^{99m}Tc-**1**. However, this potential advantage is set against disadvantage of the greater time taken to achieve the best target-to-background ratio *in vivo*. Thus, the advantages in practical use are likely to arise in situations where prolonged action are important, that is, therapeutic applications of the longer lived isotopes ^{188}Re (17 h) and ^{186}Re (90 h) rather than imaging applications of the short lived ^{99m}Tc (6 h). These advantages will be manifested if the biodistribution and kinetics of the Tc and Re analogues prove to be the same, as they have done in the case of [^{99m}Tc]-**4** and [^{188}Re]-**5**[12, 13]; preliminary *in vivo* biodistribution studies suggest that this is also the case for [^{188}Re]-**8** (see supplemental information). [^{188}Re]-**8** shows the expected and desired specificity for bone and joints and low retention in kidney, at 24 h, giving a qualitative indication of prolonged *in vivo* stability. Although quantitative comparison with other rhenium-188 bone targeting radiopharmaceuticals has not been part of this study, the data suggest that [^{188}Re]-**8** will have advantages over ^{188}Re-HEDP and warrants further evaluation as a radiopharmaceutical for radionuclide therapy of bone metastases. Thus both [^{188}Re]-**5** and [^{188}Re]-**7** are likely to offer improvements in radionuclide therapy compared to the conventional agents $^{188/186}$Re-HEDP.

^{31}P NMR and X-ray powder diffraction studies of calcified plaques from animals and humans show that the minerals present in vascular calcification closely resemble hydroxyapatite.[31] Radiolabelled bisphosphonates bind avidly with hydroxyapatite; hence they have the potential to be used as agents for imaging of vascular calcification. This prediction presupposes that the mechanism of uptake in calcified tissue and bone is through direct binding to mineral – but it could also be related to cellular transport mechanisms involving osteoclast/osteoblast-like cells involved in the calcification process, as has been implicated in the mechanism of action of bisphosphonate drugs used to treat bone disorders.[32] Nevertheless it is consistent with the observation that the tracers described here bind to the pathological mineral samples tested, and the *in vivo* results show that the tracers indeed target not only bone but also vascular soft tissue calcification. There have been previous reports of extra-osseous uptake of ^{99m}Tc-**1** linked with atherosclerosis and vascular calcification. For example DeLong *et al.* reported the visualisation of calcified femoral arteries in delayed images of patients undergoing bone scans.[33] The clinical value of imaging vascular calcification has, however, yet to be fully explored.

Conclusion

The new technetium and rhenium complexes with two pendant bisphosphonate groups have been synthesised by simple methods amenable to kit-based radiolabelling. The presence of one and two pendant bisphosphonate groups confers advantages over conventional bisphosphonate complexes in which the bisphosphonate group is involved in technetium or rhenium chelation, in terms of *in vivo* stability and affinity for hydroxyapatite of synthetic and biological origin. These advantages are likely to be

significant in therapeutic applications involving the longer half-life isotopes ^{186}Re and ^{188}Re. All three classes of ^{99m}Tc complex described here are capable of imaging vascular soft tissue calcification as well as bone disease. The tracers and biological models described here prove a means to study the diagnostic meaning and value of imaging of vascular calcification, leading to clinical applications; however, the present data do not indicate that the advantages in stability and mineral affinity displayed by the new complexes translate into practical advantages in imaging compared to conventional ^{99m}Tc-bisphosphonate tracers such as ^{99m}Tc-**1**. Finally, [^{188}Re]-**8** deserves further biological evaluation as a radiopharmaceutical for palliative treatment of bone metastases because of its high *in vivo* stability, selective uptake in bone and joints, and low retention in kidney at 24 h.

Acknowledgements

This research was supported by the Centre of Excellence in Medical Engineering funded by the Wellcome Trust and EPSRC under grant number WT088641/Z/09/Z, the Kings College London and UCL Comprehensive Cancer Imaging Centre funded by the CRUK and EPSRC in association with the MRC and DoH (England), the British Heart Foundation centre of Research Excellence at King's College London and the National Institute for Health Research (NIHR) Biomedical Research Centre at Guy's and St Thomas' NHS Foundation Trust and King's College London. The views expressed are those of the authors and not necessarily those of the NHS, the NIHR or the Department of Health. Imaging equipment used was purchased through an equipment grant from Wellcome Trust. A postdoctoral placement at King's for IUK was funded by the Higher Education Commission (HEC), Islamabad, Pakistan. We thank Rachel C. Murray of the Animal Health Trust for providing us with the equine bone sample.

References

1. G. Subramanian, J. G. McAfee, R. J. Blair, F. A. Kallfelz and F. D. Thomas, *J. Nucl. Med.*, 1975, **16**, 744-755.
2. S. Zhang, G. Gangal and H. Uludağ, *Chem. Soc. Rev.*, 2007, **36**, 507-531.
3. V. J. Lewington, *J. Nucl. Med.*, 2005, **46**, 38S-47S.
4. J. M. de Klerk, A. D. van het Schip, B. A. Zonnenberg, A. van Dijk, J. M. Quirijnen, G. H. Blijham and P. P. van Rijk, *J. Nucl. Med.*, 1996, **37**, 244-249.
5. B. T. Hsieh, J. F. Hsieh, S. C. Tsai, W. Y. Lin, S. J. Wang and G. Ting, *Nucl. Med. Biol.*, 1999, **26**, 973-976.
6. K. Liepe, J. Kropp, R. Runge and J. Kotzerke, *Br. J. Cancer*, 2003, **89**, 625-629.
7. M. C. Graham, H. I. Scher, G.-B. Liu, S. D.-J. Yeh, T. Curley, F. Daghighian, S. J. Goldsmith and S. M. Larson, *Clin. Cancer Res.*, 1999, **5**, 1307-1318.
8. A. Handeland, M. W. Lindegaard and D. E. Heggli, *Eur. J. Nucl. Med.*, 1989, **15**, 609-611.
9. S. J. Wang, W. Y. Lin, M. N. Chen, C. S. Chi, J. T. Chen, W. L. Ho, B. T. Hsieh, L. H. Shen, Z. T. Tsai, G. Ting, S. Mirzadeh and F. F. Knapp, Jr., *J. Nucl. Med.*, 1998, **39**, 1752-1757.
10. J. M. H. de Klerk, A. van Dijk, A. D. van het Schip, B. A. Zonnenberg and P. P. van Rijk, *J. Nucl. Med.*, 1992, **33**, 646-651.
11. A. P. Winterbottom and A. S. Shaw, *Clin. Radiol.*, 2009, **64**, 1-11.
12. R. T. M. de Rosales, C. Finucane, S. J. Mather and P. J. Blower, *Chem. Commun.*, 2009, 4847-4849.
13. R. Torres Martin de Rosales, C. Finucane, J. Foster, S. J. Mather and P. J. Blower, *Bioconjugate Chem.*, 2010, **21**, 811-815.
14. D. J. Berry, R. Torres Martin de Rosales, P. Charoenphun and P. J. Blower, *Mini Rev. Med. Chem.*, 2012, **12**, 1174-1183.
15. M. A. Stalteri, S. J. Parrott, V. A. Griffiths, J. R. Dilworth and S. J. Mather, *Nucl. Med. Commun.*, 1997, **18**, 870-877.
16. F. Demaimay, L. Dazord, A. Roucoux, N. Noiret, H. Patin and A. Moisan, *Nucl. Med. Biol.*, 1997, **24**, 701-705.
17. R. Pasqualini, A. Duatti, E. Bellande, V. Comazzi, V. Brucato, D. Hoffschir, D. Fagret and M. Comet, *J. Nucl. Med.*, 1994, **35**, 334-341.
18. R. Pasqualini and A. Duatti, *J. Chem. Soc., Chem. Commun.*, 1992, 1354-1355.
19. R. Torres Martin de Rosales, R. Tavaré, R. L. Paul, M. Jauregui-Osoro, A. Protti, A. Glaria, G. Varma, I. Szanda and P. J. Blower, *Angew. Chem. Int. Ed.*, 2011, **50**, 5509-5513.
20. J. Singh, K. Reghebi, C. R. Lazarus, S. E. M. Clarke, A. P. Callahan, F. F. Knapp Jr., P. J. Blower *Nucl. Med. Commun.* 1993, **14**,197-203.
21. P. J. Blower, *Nucl. Med. Commun.* 1993, **14**, 995-997.
22. M.Abkar Ali, S. E. Livingstone and D. J. Phillips. *Inorg. Chim. Acta*, 1972, **6**, 11-16.
23. R. Torres Martin de Rosales, R. Tavaré, A. Glaria, G. Varma, A. Protti and P. J. Blower, *Bioconjugate Chem.*, 2011, **22**, 455-465.
24. J. Chatt and G. A. Rowe, *J. Chem. Soc.*, 1962, 4019-4033.
25. A. Marchi, E. Marchesi, L. Marvelli, P. Bergamini, V. Bertolasi and V. Ferretti, *Eur. J. Inorg. Chem.*, 2008, **2008**, 2670-2679.
26. D. G. Reid, C. M. Shanahan, M. J. Duer, L. G. Arroyo, M. Schoppet, R. A. Brooks and R. C. Murray, *J. Lipid Res.*, 2012, **53**, 1569-1575.
27. P. A. Price, S. A. Faus and M. K. Williamson, *Arterioscler. Thromb. Vasc. Biol.*, 2000, **20**, 317-327.
28. L. J. Schurgers, H. M. H. Spronk, B. A. M. Soute, P. M. Schiffers, J. G. R. DeMey and C. Vermeer, *Blood*, 2007, **109**, 2823-2831.
29. A. Boschi, C. Bolzati, L. Uccelli, A. Duatti, *Nucl. Med. Biol.* 2003, **30**, 381-387.

30. S. J. Mather and D. Ellison, *J. Nucl. Med.*, 1990, **31**, 692-697.
31. W. Guo, J. D. Morrisett, M. E. DeBakey, G. M. Lawrie and J. A. Hamilton, *Arterioscler. Thromb. Vasc. Biol.*, 2000, **20**, 1630-1636.
32. R. G. G. Russell, *Bone*, 2007, **40**, S21-S25.
33. E. B. Silberstein and S. DeLong, *Clin. Nucl. Med.*, 1985, **10**, 738-739.

